ANL-6420

ANL-6420

Argonne National Laboratory

GEOMETRICAL CONSIDERATIONS IN THE MEASUREMENT OF THE RATIO L/R IN THE SCATTERING OF POLARIZED NUCLEONS

by

J. E. Monahan and A. J. Elwyn

ANL-6420
Physics
(TID-4500, 16th Ed., Amended)
AEC Research and Development Report

ARGONNE NATIONAL LABORATORY
9700 South Cass Avenue
Argonne, Illinois

GEOMETRICAL CONSIDERATIONS IN THE MEASUREMENT OF THE RATIO L/R IN THE SCATTERING OF POLARIZED NUCLEONS

by

J. E. Monahan and A. J. Elwyn

Physics Division

September 1961

Operated by The University of Chicago
under
Contract W-31-109-eng-38

Abstract

This report describes a FORTRAN II program which is used to evaluate the effect of a spatially extended analyzer and detector on the measurement of the left-right asymmetry in the scattering of polarized particles. In particular, the initial scatterer is assumed to be a point source and the analyzer (second scatterer) and detector are treated as planes whose dimensions are adjustable as input data in the program. The calculation also allows for any given angular distribution of particle flux from the source if this distribution can be represented as a finite power series in the cosine of the angle of emission. A similar representation is used to describe the scattering properties of the analyzer. The integrals over the finite dimensions of the analyzer and detector are evaluated by a standard Newton-Cotes quadrature approximation for multidimensional integration. A discussion of this approximation as well as a listing of the FORTRAN program are included as appendices to this report.

I. INTRODUCTION

A number of authors[1] have pointed out that the particles produced in a nuclear scattering or reaction usually are partially polarized in a plane perpendicular to the plane of the scattering or reaction. The usual method of measuring the amount of this polarization is a double-scattering experiment in which the ratio of the counting rates in two detectors* set at equal angles on opposite sides of the second scatterer (analyzer) is determined. This ratio L/R, the counting rate in the detector placed at the "left" of the direction of the beam of nucleons incident on the second scatterer divided by the rate in the one at the "right", is related to the polarization by

$$\frac{L}{R} = \frac{1 - P_1(\theta_1)\, P_2(\theta_2)}{1 + P_1(\theta_1)\, P_2(\theta_2)} \quad , \tag{1}$$

where $P_1(\theta_1)$ is the initial spin polarization of nucleons emanating from the source at an angle θ_1 with respect to the direction of incidence of an unpolarized initial beam (Fig. 1) and $P_2(\theta_2)$ is the polarization that results when an unpolarized beam of nucleons incident on the analyzer is scattered through an angle θ_2. The reaction and scattering planes at the source and at the analyzer coincide. The sign convention in Eq. (1) is based on the assumption that θ_1 is measured in a clockwise sense from the direction of incidence at the source as is indicated in Fig. 1. Furthermore, the sign of the polarization[2] at each scattering is taken to be positive in the direction of $\vec{k}_i \times \vec{k}_f$, where $\vec{k}_i$ and $\vec{k}_f$ are the respective wave numbers of the incident and outgoing particles.

As a matter of convenience in the discussion to follow, the initial

---

*Usually a single detector is used in this type of measurement. The ratio of the counting rates on the two sides of the scatterer is determined by moving the detector first to one position and then to the other.

reaction at the source is specified to be of the type A(p, n)B in which polarized neutrons result when target nuclei A are bombarded with protons. The polarized neutron beam is scattered by an analyzer and the left-right asymmetry of this second scattering is measured.

Equation (1) is strictly valid only for the idealized case in which the neutron source, the analyzer, and the detectors can be represented as geometrical points. In practice, therefore, the quantities $P_1(\theta_1)$ and $P_2(\theta_2)$, as determined by Eq. (1), represent some sort of average over the differential cross sections and over the extended dimensions of the experimental layout involved in the measurement of L/R. In order to insure a physically meaningful measurement of the product $P_1 P_2$ it is necessary to investigate the dependence of this product, as determined by Eq. (1), on the particular geometrical factors involved in any given experimental arrangement. In this report we present the results of a calculation that indicates the type of correction which must be applied to left-right asymmetry measurements in order to take into account the effects arising from the finite dimensions of the analyzer and detector, from the anisotropy of the neutron flux from the A(p, n)B source, and from the scattering properties of the analyzer. In the course of the calculation Eq. (1) is rewritten in a form such that $P_1 P_2$ is independent of the experimental layout and the quantities $P_1(\theta_1)$ and $P_2(\theta_2)$ are redefined to be the polarizations at the mean angles θ_1 and θ_2 determined by this geometric arrangement.

The general expression for the ratio L/R is derived in Sec. II for the case of a point source, finite analyzer, and finite detector. This expression is more general than those used in previous similar calculations[3] in that the analyzer and detector are treated as planes rather than approximated as points and lines. Our final equation for the measured ratio L/R involves two different families of four-dimensional integrals. These integrals are evaluated by means of a standard Newton-Cotes quadrature approximation appropriate for multidimensional integration. The details of this approximate integration are given in

Appendix I. Although the actual integrations are performed for a specific geometric configuration, namely that in which the analyzer and detector are rectangular areas, the general features of the results should be applicable to a variety of different shapes of analyzers and detectors. Furthermore, only a slight redefinition of the integration variables is required in order to obtain results for other standard experimental arrangements. In Appendix II we give the FORTRAN listing for the calculation as it was prepared for use on the IBM-704 fast digital computer at Argonne.

The numerical results of a calculation for a specific example are discussed in Sec. III, and in Sec. IV suggestions are given for possible uses of this type of calculation in other connections.

II. EFFECTS OF THE EXPERIMENTAL CONFIGURATION ON THE MEASURED RATIO L/R

The experimental arrangement which is of primary concern in this report has been utilized previously at Argonne to study the angular distributions of neutrons scattered from various nuclei.[4] The same setup, with slight modifications, is now being used to study the scattering of polarized neutrons.[5] These calculations were occasioned by this latter type of experiment.

The neutron detectors are arrays of BF_3 counters in an oil moderator, surrounded by large shield tanks which are filled with borated water. Neutrons scattered by the analyzer enter the detectors by passing through rectangular collimating holes cut in the shield. The detectors ride on a circular track, with their collimators pointing toward a rectangular slab-shaped scattering sample at its center. This sample serves as an analyzer in the present experiments. The analyzer is "illuminated" by a rectangular conically-collimated beam of neutrons from a "point source" located at the center of a shielded source tank. The neutrons are produced in (p, n) reactions, the protons being accelerated in the Argonne

4-Mev Van de Graaff accelerator.*

In this section an expression for the ratio L/R is derived without specific reference to an actual geometric arrangement. However, the FORTRAN program listed in Appendix II is applicable only to the slab-shaped analyzer and detectors described above.

The experimental arrangement is shown schematically in Fig. 1. With reference to this figure the symbols used in the derivation are defined as follows. Unpolarized protons are incident on a point source S at the origin of the (X, Y, Z) coordinate system. The direction of incidence of these particles is denoted by the unit vector $\hat{r}_0$ with direction cosines $(0, -\sin\theta_1, \cos\theta_1)$. The protons initiate a reaction at S, giving rise to neutrons which are emitted along a direction $\vec{r}_1 / |\vec{r}_1|$. This direction makes an angle β with the direction of incidence of the proton beam. The polarization of this neutron beam is denoted by $\vec{P}_1(\beta)$. A scattering target (analyzer) T is located such that its center is at the point $(0, 0, \ell_1)$ in the (X, Y, Z) coordinate system.

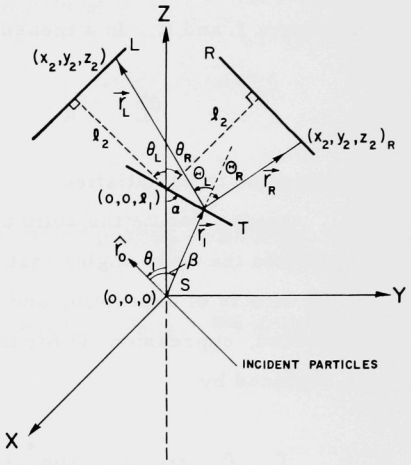

Fig. 1. Schematic diagram defining the symbols used in discussing the situation in which neutrons from point source S are scattered from a slab-shaped scattering target (analyzer) T and are counted by slab-shaped detectors L and R. Protons inducing the (p, n) reaction at S are incident in the direction of unit vector $\hat{r}_0$. The neutrons are emitted along paths such as $\vec{r}_1$ and are scattered at T along such paths as $\vec{r}_L$ and $\vec{r}_R$.

*A more thorough description of this experimental setup may be found in reference 4.

This target is skewed such that its normal makes an angle $\frac{\pi}{2} - \alpha$ with respect to the positive Z axis. The neutrons scatter from T through the angles Θ_R and Θ_L and move along the vectors $\vec{r}_R$ and $\vec{r}_L$ to the detectors R and L, respectively. The detectors are oriented so that their center points lie in the (Y, Z) plane at a perpendicular distance ℓ_2 from the point $(0, 0, \ell_1)$ on T. The symbols θ_L and θ_R denote respectively the mean scattering angles determined by the center points of the analyzer T and of the detectors L and R. In a measurement of the ratio L/R the condition

$$\theta_L = -\theta_R , \qquad 0 \leq \theta_R \leq \pi$$

is assumed to be satisfied.

Let Ω_T denote the solid angle that T subtends at S and let Ω_L and Ω_R denote the solid angles that L and R subtend at an arbitrary point on T. If the effects of absorption and multiple scattering within the sample T are neglected, expression (1) for the ratio of the counting rates in the detectors is replaced by

$$\frac{L}{R} = \frac{\int_{\Omega_T}\int_{\Omega_L} d\Omega_T\, d\Omega_L\, N(\beta, \alpha)\, \sigma_1(\beta)\, \sigma_2(\Theta_L)\, [1 + \vec{P}_1(\beta) \cdot \vec{P}_2(\Theta_L)]}{\int_{\Omega_T}\int_{\Omega_L} d\Omega_T\, d\Omega_R\, N(\beta, \alpha)\, \sigma_1(\beta)\, \sigma_2(\Theta_R)\, [1 + \vec{P}_1(\beta) \cdot \vec{P}_2(\Theta_R)]} . \qquad (2)$$

Here $\sigma_1(\beta)$ is the differential cross section for the (p, n) reaction at S, $\sigma_2(\Theta)[1 + \vec{P}_1(\beta) \cdot \vec{P}_2(\Theta)]$ is the differential cross section for the scattering of a polarized neutron beam from the analyzer T, and $N(\beta, \alpha)$ is the relative thickness of the analyzer as measured in the direction of incidence. The vector $\vec{P}_2(\Theta)$ is the polarization that would result if an unpolarized beam incident on T was scattered through an angle Θ at T.

In order to carry out the integrations indicated in Eq. (2) for the rectangular analyzer and detectors described above, it is convenient to

introduce the coordinates (γ,ϵ) in the plane of the analyzer T by means of the transformation

$$(x_1, y_1, z_1) \longrightarrow (\gamma, \epsilon \sin\alpha, \ell_1 - \epsilon \cos\alpha) \quad , \tag{3a}$$

where (x_1, y_1, z_1) is any point on T. Similarly we define coordinates (η, ξ) in the planes of the detectors by the transformations

$$(x_2, y_2, z_2)_R \longrightarrow (\eta, \ell_2 \sin\theta_R + \xi \cos\theta_R, \ell_1 + \ell_2 \cos\theta_R - \xi \sin\theta_R) \quad , \tag{3b}$$

and

$$(x_2, y_2, z_2)_L \longrightarrow (\eta, -\ell_2 \sin\theta_R + \xi \cos\theta_R, \ell_1 + \ell_2 \cos\theta_R + \xi \sin\theta_R) \quad , \tag{3c}$$

where $(x_2, y_2, z_2)_{R,\,L}$ denote points on the detectors R, L. We introduce these transformations into Eq. (2) to obtain

$$\frac{L}{R} = \frac{\int d\gamma \int d\epsilon \int d\xi \int d\eta \, (\hat{n}_T \cdot \vec{r}_1 / r_1^3) \, N(\alpha,\beta) \, G_L}{\int d\gamma \int d\epsilon \int d\xi \int d\eta \, (\hat{n}_T \cdot \vec{r}_1 / r_1^3) \, N(\alpha,\beta) \, G_R} \quad , \tag{4}$$

$$G_D = (\hat{n}_D \cdot \vec{r}_D / r_D^3) \, \sigma_2(\Theta_D) [1 + P_1(\beta) \, P_2(\Theta_D) \, \hat{n}_1 \cdot \hat{n}_2] \quad ,$$

where D represents either L or R and

$$N(\alpha,\beta) = \frac{r_1}{y_1 \cos\alpha + z_1 \sin\alpha} \quad ,$$

$$\hat{r}_1 = (\hat{x} x_1 + \hat{y} y_1 + \hat{z} z_1)/r_1 \quad ,$$

$$r_1^2 = x_1^2 + y_1^2 + z_1^2 \quad ,$$

$$\hat{r}_{R,L} = [\hat{x}(x_2 - x_1) + \hat{y}(y_2 - y_1) + \hat{z}(z_2 - z_1)] / r_{R,L} \quad ,$$

$$r_{R,L}^2 = (x_2 - x_1)^2 + (y_2 - y_1)^2 + (z_2 - z_1)^2 \quad ,$$

$$\hat{r}_0 = -\hat{y}\sin\theta_1 + \hat{z}\cos\theta_1 \quad ,$$

$$\hat{n}_1 = \hat{r}_0 \times \hat{r}_1 / |\hat{r}_0 \times \hat{r}_1| = \hat{r}_0 \times \hat{r}_1 / |\sin\beta| \quad ,$$

$$\hat{n}_2 = \hat{r}_1 \times \hat{r}_{R,L} / |\hat{r}_1 \times \hat{r}_{R,L}| = \hat{r}_1 \times \hat{r}_{R,L} / |\sin\Theta_{R,L}| \quad ,$$

$$\hat{n}_{R,L} = \hat{y}\sin\theta_{R,L} + \hat{z}\cos\theta_{R,L} \quad ,$$

$$\hat{n}_T = \hat{y}\cos\alpha + \hat{z}\sin\alpha$$

and

$$\cos\Theta_{R,L} = \hat{r}_1 \cdot \hat{r}_2 \quad ,$$

$$\cos\beta = \hat{r}_0 \cdot \hat{r}_1 \quad .$$

The quantities with the carets are unit vectors in the directions indicated. We have omitted the subscripts R and L from the coordinates (x_2, y_2, z_2) in these relations. The triad $(\hat{x}, \hat{y}, \hat{z})$ denotes a set of unit vectors along the axes of the (X, Y, Z) coordinate system. These rectangular coordinates are given in terms of the integration variables by Eqs. (3). The use of the notation $\hat{n}_2$ for two different quantities in Eq. (4) causes no confusion since the numerator of this expression refers to the L counter

and the denominator to the R counter.

The generality of the present derivation is retained by expanding the cross sections and polarizations occurring in Eq. (4) in the form

$$\sigma_1(\beta) = \sum_{n=0}^{2\ell} A_n \cos^n\beta, \qquad \sigma_1(\beta) P_1(\beta) = \sum_{n=0}^{2\ell - 1} a_n \cos^n\beta \sin\beta \ ,$$

$$\sigma_2(\Theta) = \sum_{k=0}^{2\ell'} B_k \cos^k\Theta \ , \qquad \sigma_2(\Theta) P_2(\Theta) = \sum_{k=0}^{2\ell'-1} b_k \cos^k\Theta \sin\Theta \ , \tag{5}$$

where ℓ and ℓ' denote the maximum values of the orbital angular momentum associated with each reaction.

In an experiment one would like to obtain an expression for the polarization product (evaluated at the nominal mean angles set by the apparatus) in terms of the measured ratio L/R. This can be accomplished most simply by introducing a correction factor ρ, which serves to correct Eq. (2) for these effects of finite size. We write

$$\frac{L}{R} = \rho \, \frac{1 - P_1(\theta_1) P_2(\theta_2)}{1 + P_1(\theta_1) P_2(\theta_2)} \ , \tag{6}$$

where $\theta_2 = \theta_R = -\theta_L$. After the explicit introduction of the expansions (5), a comparison of Eqs. (4) and (6) gives

$$\rho = \frac{\mathcal{I}(L) + \mathcal{M}(L)}{\mathcal{I}(R) + \mathcal{M}(R)} \left(\frac{\mathcal{D}_1 + \mathcal{D}_2}{\mathcal{D}_1 - \mathcal{D}_2} \right), \tag{7}$$

where

$$\mathcal{I}(L, R) = \sum_{n=0}^{2\ell} \sum_{k=0}^{2\ell'} A_n B_k I_{n,k}(L, R) \ ,$$

$$\mathcal{M}(L, R) = \sum_{n=0}^{2\ell-1} \sum_{k=0}^{2\ell'-1} a_n b_k M_{n,k}(L, R) \quad ,$$

$$\mathcal{D}_1 = \sum_{n=0}^{2\ell} \sum_{k=0}^{2\ell'} A_n B_k \cos^n\theta_1 \cos^k\theta_2 \quad ,$$

and

$$\mathcal{D}_2 = \sum_{n=0}^{2\ell-1} \sum_{k=0}^{2\ell'-1} a_n b_k \cos^n\theta_1 \cos^k\theta_2 \sin\theta_1 \sin\theta_2 \quad .$$

The symbols $I_{n,k}$ and $M_{n,k}$ denote the integrals

$$I_{n,k}(R, L) = \int_T \int d\gamma d\epsilon \int_{R,L} \int d\xi d\eta \frac{\hat{n}_T \cdot \vec{r}_1}{r_1^3} \frac{\hat{n}_{L,R} \cdot \vec{r}_{L,R}}{r_{R,L}^3}$$

$$\times N(\alpha, \beta) \cos^n\beta \cos^k\Theta_{R,L} \quad , \tag{8a}$$

and

$$M_{n,k}(R, L) = \int_T \int d\gamma d\epsilon \int_{R,L} \int d\xi d\eta \frac{\hat{n}_T \cdot \vec{r}_1}{r_1^3} \frac{\hat{n}_{L,R} \cdot \vec{r}_{L,R}}{r_{R,L}^3} (\hat{n}_1 \cdot \hat{n}_2)$$

$$\times N(\alpha, \beta) \cos^n\beta \cos^k\Theta_{R,L} \sin\beta \sin\Theta_{R,L} \quad . \tag{8b}$$

The integrations in Eqs. (8) are to be performed over the illuminated area T of the analyzer and over the sensitive area R or L of the detectors. The limits on the integrals are to be measured in the planes of the analyzer and detector. Appendix I discusses the method of numerical integration used to evaluate these integrals. Appendix II describes the FORTRAN program used, for a given geometric arrangement, to evaluate the inte-

grals (8) for a sequence of values of n and k. Once these integrals have been determined, the factor ρ can be evaluated in terms of the coefficients that determine the differential cross sections for polarized and unpolarized nucleons.

The actual evaluation of the factor ρ requires, of course, knowledge of the angular dependence of the cross sections appearing in Eq. (3). This presupposed information is, in fact, more detailed than that which is being measured. However, the values of the integrals in Eqs. (8) are not dependent on any details of these cross sections and once these are evaluated for a particular experimental setup it is usually possible to determine the magnitude of ρ by the use of a reasonable approximation to the form of the angular distributions. An illustration of this is given in Sec. III of this report. From such approximations it is possible to determine whether a modification of the experimental setup is necessary.

III. A NUMERICAL EXAMPLE

The use of the method discussed above is illustrated in this section by detailing the results of a particular numerical calculation. The parameters that are used are those that describe the experimental setup for the Argonne polarization measurements.[5] In terms of symbols defined previously these are: $\ell_1 = 59$ inches, $\ell_2 = 82.5$ inches, $\alpha = 90^\circ$, $\theta_1 = 51^\circ$, and $\theta_2 = \theta_R = -\theta_L = 45^\circ$. The "illuminated" area* of the analyzer T is a 4×16-inch rectangle (as measured in the plane of T), and the sensitive area of each detector is a 6×16-inch rectangle. Thus the ranges of integration in Eqs. (8) are

$$-2 \leq \epsilon \leq 2, \quad -8 \leq \gamma \leq 8, \quad -3 \leq \xi \leq 3, \quad -8 \leq \eta \leq 8 \quad .$$

---

*In general the limits of the ϵ integration depend on the angle α. For $\alpha = \pi/2$, however, this dependence cancels and the limits are simply the dimensions of the neutron beam at T. The case in which $\alpha \neq \pi/2$ is discussed in Appendix II.

The quantities listed above serve as input data to the FORTRAN program. The data sheet, Table II, appropriate to this example as well as the "program output", Table III, namely the numerical values of the integrals in Eqs. (8), are included in Appendix II of this report.

If we assume that the conditions $2\ell \leq 2$ and $2\ell' \leq 2$ are satisfied, the expansion (5) for the cross sections have the forms

$$\sigma_1(\beta) = A_0 + A_1 \cos\beta + A_2 \cos^2\beta \quad , \tag{9a}$$

$$\sigma_1(\beta)P_1(\beta) = a_0 \sin\beta + a_1 \cos\beta \sin\beta \quad , \tag{9b}$$

$$\sigma_2(\Theta) = B_0 + B_1 \cos\Theta + B_2 \cos^2\Theta \quad , \tag{9c}$$

$$\sigma_2(\Theta)P_2(\Theta) = b_0 \sin\Theta + b_1 \cos\Theta \sin\Theta \quad . \tag{9d}$$

In terms of these coefficients and the results of the numerical evaluation of the integrals as given in Table III, Appendix II the correction factor, Eq. (7), becomes

$$\rho = \frac{1 - 10^{-2}a/(d_1 - d_2)}{1 - 10^{-2}b/(d_1 + d_2)} \quad , \tag{10}$$

where

$$a = (0.16A_1 + 0.20A_2)\,B_0 + (0.89A_0 + 0.66A_1 + 0.45A_2)\,B_1$$
$$+ (1.18A_0 + 0.80A_1 + 0.52A_2)\,B_2$$
$$+ (0.33a_0 + 0.08a_1)\,b_0 - (0.35a_0 + 0.29a_1)\,b_1 \quad ,$$

$$b = (0.21A_1 + 0.25A_2)\,B_0 + (0.89A_0 + 0.76A_1 + 0.59A_2)\,B_1$$
$$+ (1.18A_0 + 0.90A_1 + 0.67A_2)\,B_2$$
$$+ (0.81a_0 + 0.65a_1)\,b_0 + (1.09a_0 + 0.78a_1)\,b_1 \quad ,$$

$$d_1 = (A_0 + 0.63A_1 + 0.40A_2)B_0 + (0.71A_0 + 0.45A_1 + 0.28A_2)B_1 + (0.50A_0 + 0.32A_1 + 0.20A_2)B_2 \ ,$$

$$d_2 = (0.55a_0 + 0.35a_1)b_0 + (0.39a_0 + 0.25a_1)b_1 \ .$$

In this type of experiment, information usually is available concerning the angular scattering and polarization properties either of the source S or of the analyzer T. In the present example we assume that the analyzer is a slab of natural magnesium and that the neutron source is the $Li^7(p, n)Be^7$ reaction. At a proton energy E_p of approximately 2.28 Mev, the resultant neutrons emerging at 51° with respect to the direction of incidence of the proton beam have an energy of about 0.43 Mev. The differential cross section and polarization of neutrons scattered by magnesium at this energy have been measured[6] and are given approximately by Eqs. (9c) and (9d), where

$$B_0 = 0.62, \quad B_1 = 0.40, \quad B_2 = 0.76,$$

and

$$b_0 = 0.36, \quad b_1 = 1.16.$$

For $E_p \approx 2.28$ Mev, the differential cross section for the $Li^7(p, n)Be^7$ reaction is represented in the laboratory system by Eq. (9a) when the coefficients* have the values

$$A_0 = 0.029, \quad A_1 = 0.041, \quad A_2 = 0.021 \ .$$

---

*These coefficients were obtained from those given by R. Taschek and A. Hemmendinger, Phys. Rev. 74, 373 (1948). In this reference the coefficients are reported in terms of coefficients in a Legendre-polynomial expansion of the cross section relative to the center-of-mass system of coordinates. Thus it was necessary to transform into the representation used above, viz., a power-series expansion in terms of cosines in the laboratory coordinate system.

For these values of the cross-section coefficients the quantities defined by the relations following Eq. (10) become

$$a = 0.09 - 0.29a_0 - 0.31a_1 ,$$

$$b = 0.10 + 1.56a_0 + 1.14a_1 ,$$

$$d_1 = 0.08 ,$$

$$d_2 = 0.65a_0 + 0.41a_1 .$$

As stated previously, the values of the polarization coefficients a_0 and a_1 could be obtained only from considerably more detailed measurements than any being made. Consequently it is unreasonable to assume that these data are available for the evaluation of ρ. Fortunately, at least for the experimental arrangement considered here, the correction factor is not particularly sensitive to the precise values of a_0 and a_1, at least within the range of values which are physically possible for these coefficients.

This can be shown by use of the fact that by definition of the polarization we have

$$|P_2(\Theta)| \leq 1 \quad , \quad 0 \leq \Theta \leq \pi .$$

This condition in conjunction with Eqs. (9a) and (9b) shows that the undetermined polarization coefficients must satisfy the inequalities

$$|a_0| \leq A_0$$

and

$$|a_1| \leq 2[A_0 - \frac{1}{\sqrt{2}}|A| + \frac{1}{2}A_2] \qquad \text{if} \quad a_0 a_1 < 0$$

$$|a_1|^2 - 2\sqrt{2}\,A_0|a_1| \leq [A_0 - \frac{1}{\sqrt{2}}|A_1| + \frac{1}{2}A_2]^2 \qquad \text{if} \quad a_0 a_1 > 0 .$$

In the case which we are considering, these conditions become

$$-0.03 \leq a_0 \leq 0.03,$$

and

$$-0.08 \leq a_1 \leq 0.08 .$$

For values of these coefficients within this range it is possible to show that the value of ρ, Eq. (10), satisfies the inequality

$$|1 - \rho| \leq 0.04 .$$

Thus for this determination of the polarization $P_1(51^\circ)$ associated with the $Li^7(p, n)$ reaction at $E_p \approx 2.28$ Mev, the correction due to geometric factors is 4% at most.

If the polarization $P_1(\beta)$ in the Li(p, n) reaction is assumed to vary as $\sin\beta$, measurements[5, 7] of the neutron polarization indicate that the quantity $P_1(\beta)\sigma_1(\beta)$ has approximately the form of Eq. (9b), where

$$a_0 = -0.015 , \qquad a_1 = -0.03 .$$

For these values the correction factor ρ is found to have the value 0.997.

IV. DISCUSSION

Further calculations have been made for different values of ℓ_1 and ℓ_2 but with all other geometrical and cross-section parameters fixed at the values listed in Sec. III. In particular, ℓ_2 was fixed at a value of 10 inches and ρ was evaluated for ℓ_1 equal to 20, 6, and 2 inches. Decreasing ℓ_1 from 20 to 2 inches corresponds to about a 40-fold increase in the solid angle the Mg analyzer subtended at the neutron source. This increase in solid angle resulted in a decrease in the value of the correction

factor ρ. On the other hand, in exactly the same experimental arrangement but with all angular distribution coefficients set equal to each other, i.e., with

$$A_0 = A_1 = A_2 = B_0 = B_1 = B_2 = a_0 = a_1 = b_0 = b_1 \quad ,$$

the value of ρ was found to increase as the solid angle of the analyzer was increased. The actual values of ρ calculated for these parameters are given in Table I.

TABLE I. Values of ρ calculated for different parameters in the experimental arrangement involving slab-shaped scatterers and detectors described in Sec. III. The areas of scatterer and detectors are the same as in the calculation of Sec. III. In Case A the coefficients describing the cross sections are the same as those used in the calculations in Sec. III. In Case B these coefficients are assumed equal to each other.

ℓ_1 (inches)	ℓ_2 (inches)	ρ	
		Case A	Case B
20	10	0.933	1.082
6	10	0.942	1.123
2	10	0.992	1.623

These results serve to emphasize that, in experiments of the type discussed here, the scattering (or reaction) properties of the source and analyzer are highly correlated with each other and with the sizes and positions of the analyzer and detectors. Because of the complexity of these correlations, it is obviously impossible to draw any general conclusions concerning the magnitude of the correction factor ρ. Even

for a specified experimental arrangement it is necessary to limit the complexity of the relevant cross sections before a reasonable estimate of the value of this correction factor can be made. It is obvious that so many sets of conditions are experimentally realizable that no comprehensive survey of the behavior of ρ is possible. The program and methods described above, however, may be of value in the assessment of the error to be expected as a result of the layout of a proposed experiment.

Although the present calculations are limited to the special case of a rectangular-slab analyzer and a rectangular detector, the program should be applicable to other experimental arrangements. For example, in so far as attenuation and multiple-scattering can be neglected, the present methods of integration should be applicable to analyzers and detectors in the form of cylinders, at least for those cases in which ℓ_1 and ℓ_2 are large compared with the diameters of the cylinders.

This type of calculation also has use as a tool in the determination of the most suitable geometrical arrangement for left-right asymmetry measurements and as an aid in the alignment of the experimental apparatus. Suppose, for example, that one knows the distribution of flux incident on an analyzer and that the material used as analyzer shows no polarization effects at the energy of interest. One then can calculate the extent of the left-right asymmetry that can be attributed solely to geometrical effects. The results of the calculation will indicate whether a modification in the experimental setup is necessary, and a comparison of the calculated and measured ratios L/R will indicate any possible misalignment.

As has been pointed out by a number of authors,[1,3] the instrumental asymmetries in these left-right intensity measurements can be avoided entirely by using a magnetic field between the neutron source and the analyzer to cause the neutron spin to precess through π radians. (An electromagnet is being used at the present time at Argonne in the study of neutron polarization.) Even in this case, however, it is desirable to know how the nominal mean angle of scattering set by the experimental

arrangement compares with the "true" mean angle. Actually a "true" mean angle cannot be defined without reference to the specific cross sections of the source and analyzer. However, a general result can be obtained if the mean cosines of the angle of scatter are defined by

$$\left\langle \cos^{p}\theta \right\rangle_{Av} = \frac{I_{0p}}{I_{00}} \quad .$$

With these definitions, the integrals of Eq. (8a) allow a proper series expansion of all relevant cross sections in terms of the "true" angle of scatter. This point is discussed in detail in reference 4.

APPENDIX I. A QUADRATURE APPROXIMATION IN FOUR-DIMENSIONAL INTEGRATION

Each of the integrals considered in this report can be written in the form

$$\mathcal{J} = \int_{\gamma_0}^{\Gamma} d\gamma \int_{\epsilon_0}^{E} d\epsilon \int_{\eta_0}^{H} d\eta \int_{\xi_0}^{\bar{\xi}} d\xi \; F(\gamma, \epsilon, \eta, \xi) \quad , \tag{I. 1}$$

where F is any one of the functions in Eqs. (8a) and (8b). For a given range $\mathcal{R}$ of the integration variables, we wish to obtain a numerical approximation, say I, to the value of $\mathcal{J}$. The method that is used is the standard Newton-Cotes quadrature approximation extended to the treatment of multidimensional integrals. Since this extension is not considered in the standard texts on numerical methods, it is given here in some detail.

The general method of approximation is quite simple. The region $\mathcal{R}$ of integration is subdivided into a number of nonoverlapping subregions, in each of which the function F is approximated by a polynomial Φ_n of the form

$$\Phi_n(\gamma,\epsilon,\eta,\xi) = \sum_{\lambda,\mu,\nu,\sigma=0}^{n} a_{\lambda\mu\nu\sigma} \prod_{\alpha=1}^{\lambda} (\gamma - \gamma_{\alpha-1}) \prod_{\beta=1}^{\mu} (\epsilon - \epsilon_{\beta-1}) \prod_{\gamma=1}^{\nu} (\eta - \eta_{\gamma-1})$$

$$\times \prod_{\rho=1}^{\sigma} (\xi - \xi_{\rho-1}) \quad , \tag{I. 2}$$

where the coefficients $a_{\lambda\mu\nu\sigma}$ are required to satisfy the conditions

$$\Phi_n(\gamma_p, \epsilon_r, \eta_s, \xi_t) = F_{p,r,s,t} \quad , \qquad (\gamma_p, \epsilon_r, \eta_s, \xi_t) \in \mathfrak{R} \, . \tag{I. 3}$$

In Eq. (I. 3) we have introduced the notation

$$F_{p,r,s,t} = F(\gamma_p, \epsilon_r, \eta_s, \xi_t) \, . \tag{I. 4}$$

The approximate value I of $\mathcal{I}$ is determined by carrying out the integration of the polynomial Φ_n in each subregion and adding the results. The following derivation applies to one such subregion of $\mathfrak{R}$. The specific division of $\mathfrak{R}$ into subregions and an error estimation for this approximation are discussed in Appendix II.

The development of the method is complicated by an unavoidably tedious formalism which we proceed to introduce. If the points $(\gamma_p, \epsilon_r, \eta_s, \xi_t)$ are chosen such that

$$\gamma_{p+1} = \gamma_p + h, \quad \epsilon_{r+1} = \epsilon_r + k, \quad \eta_{s+1} = \eta_s + \ell, \quad \xi_{t+1} = \xi_t + m,$$

then

$$\prod_{\alpha=1}^{\lambda} (\gamma_p - \gamma_{\alpha-1}) = \begin{cases} h^\lambda p!/(p-\lambda)! \, , & \lambda \leq p \\ 0 \, , & \lambda > p \, , \end{cases}$$

with similar results for the other products in Eq. (I. 2). For points determined by these conditions, Eq. (I. 2) can be rewritten in the form

$$\Phi_n(\gamma_p, \epsilon_r, \eta_s, \xi_t) = \sum_{\lambda,\mu,\nu,\sigma=0}^{p,r,s,t} a_{\lambda\mu\nu\sigma} h^\lambda k^\mu \ell^\nu m^\sigma \frac{p!\, r!\, s!\, t!}{(p-\lambda)!\,(r-\mu)!\,(s-\nu)!\,(t-\sigma)!} \,. \quad \text{(I. 5)}$$

In order to evaluate the coefficients $a_{\lambda\mu\nu\sigma}$ in terms of values at specified points of the given function F, it is convenient to define the displacement operators E_κ, where

$$E_\gamma F_{p,r,s,t} = F_{p+1,r,s,t}\,, \qquad E_\epsilon F_{p,r,s,t} = F_{p,r+1,s,t}\,,$$

$$E_\eta F_{p,r,s,t} = F_{p,r,s+1,t}\,, \qquad E_\xi F_{p,r,s,t} = F_{p,r,s,t+1}\,,$$

as well as the difference operators $\Delta^{\lambda\mu\nu\sigma}$, where

$$\Delta^{\lambda\mu\nu\sigma} \equiv (E_\gamma - 1)^\lambda (E_\epsilon - 1)^\mu (E_\eta - 1)^\nu (E_\xi - 1)^\sigma \,.$$

In terms of these operators we have

$$\begin{aligned} F_{p,r,s,t} &= E_\gamma^{\,p} E_\epsilon^{\,r} E_\eta^{\,s} E_\xi^{\,t} F_{0,0,0,0} \\ &= \sum_{\lambda,\mu,\nu,\sigma=0}^{p,r,s,t} \binom{p}{\lambda}\binom{r}{\mu}\binom{s}{\nu}\binom{t}{\sigma} \Delta^{\lambda\mu\nu\sigma} F_{0,0,0,0} \,. \end{aligned} \quad \text{(I. 6)}$$

Comparing this result with Eq. (I. 5), we see that the conditions expressed in Eq. (I. 4) are satisfied provided the coefficients $a_{\lambda\mu\nu\sigma}$ are chosen to be

$$a_{\lambda\mu\nu\sigma} = \frac{\Delta^{\lambda\mu\nu\sigma} F_{0,0,0,0}}{\lambda!\mu!\nu!\sigma! h^{\lambda} k^{\mu} \ell^{\nu} m^{\sigma}} ,$$

provided that the inequality

$$\max(p,r,s,t) \leq n$$

holds. Here n is the degree of the polynomial Φ_n.

Let us define the approximate integral I_n by the expression

$$I_n = \int_{\gamma_0}^{\Gamma} d\gamma \int_{\epsilon_0}^{E} d\epsilon \int_{\eta_0}^{H} d\eta \int_{\xi_0}^{\Xi} d\xi \; \Phi_n(\gamma,\epsilon,\eta,\xi) .$$

Further, we introduce the new integration variables g, e, o, and z, where

$$gh = \gamma - \gamma_0, \quad ke = \epsilon - \epsilon_0, \quad \ell o = \eta - \eta_0, \quad mz = \xi - \xi_0 .$$

We then have

$$\gamma - \gamma_{\lambda} = h(g - \lambda), \qquad \lambda = 0, \ldots, p ,$$

$$\epsilon - \epsilon_{\mu} = k(e - \mu), \qquad \mu = 0, \ldots, r ,$$

$$\eta - \eta_{\nu} = \ell(o - \nu), \qquad \nu = 0, \ldots, s ,$$

$$\xi - \xi_{\sigma} = m(z - \sigma), \qquad \sigma = 0, \ldots, t .$$

In terms of these variables, the integral I_n can be written as

$$I_n = \int_0^{(\Gamma-\gamma_0)/h} hdg \int_0^{(E-\epsilon_0)/k} kde \int_0^{(H-\eta_0)/\ell} \ell do \int_0^{(\Xi-\xi_0)/m} mdz \; \Phi_n(g, e, o, z) , \qquad (I.7)$$

where

$$\Phi_n(g,e,o,z) = \sum_{\lambda,\mu,\nu,\sigma=0}^{n} \frac{\Delta^{\lambda\mu\nu\sigma} F_{0,0,0,0}}{\lambda!\,\mu!\,\nu!\,\sigma!} \prod_{\alpha=1}^{\lambda} (g-\alpha+1) \prod_{\beta=1}^{\mu} (e-\beta+1)$$

$$\times \prod_{\gamma=1}^{\nu} (o-\gamma+1) \prod_{\rho=1}^{\sigma} (z-\rho+1) \quad .$$

The increments h, k, ℓ, and m are determined by preassigning integers q_γ, q_ϵ, q_η, q_ξ in terms of which

$$h = (\Gamma-\gamma_0)/q_\gamma, \quad k = (E-\epsilon_0)/\gamma_\epsilon, \quad \ell = (H-\eta_0)/q_\eta, \quad m = (\Xi-\xi_0)/q_\xi \quad .$$

In order that all points at which the integrandneeds be evaluated lie within the limits of integration it is necessary that

$$n \leq \min (q_\gamma, q_\epsilon, q_\eta, q_\xi) \quad . \tag{I. 8}$$

Perform the indicated integrations in Eq. (I. 7) and make use of the expansion

$$\Delta^{\lambda\mu\nu\sigma} F_{0,0,0,0} = \sum_{a,b,c,d=0}^{\lambda,\mu,\nu,\sigma} (-1)^{a+b+c+d} \binom{\lambda}{a} \binom{\mu}{b} \binom{\nu}{c} \binom{\sigma}{d}$$

$$\times E_\gamma^{\lambda-a} E_\epsilon^{\mu-b} E_\eta^{\nu-c} E_\xi^{\sigma-d} F_{0,0,0,0} \,,$$

where

$$E_\gamma^{\lambda-a} E_\epsilon^{\mu-b} E_\eta^{\nu-c} E_\xi^{\sigma-d} F_{0,0,0,0} = F_{\lambda-a,\,\mu-b,\,\nu-c,\,\sigma-d} \quad .$$

Then we obtain

$$I_n = \sum_{p,r,s,t=0}^{n} F_{p,r,s,t}\ \beta_{p,r,s,t} \quad , \tag{I. 9}$$

where

$$\beta_{p,r,s,t} = \frac{(-1)^{p+r+s+t}\ h\,k\,\ell\,m}{p!\ r!\ s!\ t!} \sum_{\lambda=p}^{n} \frac{(-1)^{\lambda}}{(\lambda-p)!}\ Q_{\lambda}^{(\gamma)} \sum_{\mu=r}^{n} \frac{(-1)^{\mu}}{(\mu-r)!}\ Q_{\mu}^{(\epsilon)}$$

$$\times \sum_{\nu=s}^{n} \frac{(-1)^{\nu}}{(\nu-s)!}\ Q_{\nu}^{(\eta)} \sum_{\sigma=\rho}^{n} \frac{(-1)^{\sigma}}{(\sigma-\rho)!}\ Q_{\sigma}^{(\xi)} \quad ,$$

and

$$Q_{\lambda}^{(\gamma)} = \int_0^{q_\lambda} dg \prod_{a=1}^{\lambda} (g-a+1) \quad ,$$

with similar expression for $Q_{\mu}^{(\epsilon)}$, $Q_{\nu}^{(\eta)}$, and $Q_{\sigma}^{(\xi)}$.

APPENDIX II. THE INTEGRATION PROGRAM

Each of the integrals to be evaluated is expanded in the form

$$\int_{-\gamma}^{\gamma} d\gamma \int_{-\epsilon}^{\epsilon} d\epsilon \int_{-\eta}^{\eta} d\eta \int_{-\xi}^{\xi} d\xi\ F(\gamma,\epsilon,\eta,\xi) = \sum_{\lambda,\mu,\nu,\sigma=1}^{N_\gamma,N_\epsilon,N_\eta,N_\xi} \mathcal{A}(N_\gamma,N_\epsilon,N_\eta,N_\xi) \quad , \tag{II. 1}$$

where N_γ, N_ϵ, N_η, N_ξ are arbitrarily assigned positive integers and

$$\mathcal{Q}(N_\gamma, N_\epsilon, N_\eta, N_\xi) = \int_{L(\bar{\gamma})}^{U(\bar{\gamma})} d\gamma \int_{L(\bar{\epsilon})}^{U(\bar{\epsilon})} d\epsilon \int_{L(\bar{\eta})}^{U(\bar{\eta})} d\eta \int_{L(\bar{\xi})}^{U(\bar{\xi})} d\xi \; F(\gamma, \epsilon, \eta, \xi) \; . \qquad \text{(II. 2)}$$

In Eq. (II. 2) the limits are defined by

$$L(\bar{\gamma}) = -\bar{\gamma} + \frac{\lambda - 1}{N_\gamma} (2\bar{\gamma}) \quad ,$$

and

$$U(\bar{\gamma}) = -\bar{\gamma} + \frac{\lambda}{N_\gamma} (2\bar{\gamma}) \quad ,$$

with similar definitions for the limits of the other variables of integration.

The FORTRAN program which is described in this appendix approximates the integrals in Eq. (II. 2) by the method discussed in Appendix I and carries out the summation indicated in Eq. (II. 1). The integration net for each subregion of integration is determined by the choice

$$q_\gamma = q_\epsilon = q_\eta = q_\xi = 2 \; .$$

The degree n of the approximation polynomial Φ_n is taken equal to 2, consistent with the restriction expressed in Eq. (I. 8).

The input data for the program are supplied on the following punched cards:

(1) The first data card consists of six floating-point fields, each of width 12, and an implied decimal point is included between the sixth and seventh columns in each field if it is not explicitly punched elsewhere. The six fields contain the numerical values of ℓ_1, ℓ_2, $\bar{\gamma}$, $\bar{\epsilon}, \bar{\eta}$, and $\bar{\xi}$ in this sequence. Here ℓ_1 and ℓ_2 denote the distances from source to analyzer and from analyzer to detector, respectively, and $2\bar{\gamma}$, $2\bar{\epsilon}$, $2\bar{\eta}$, and $2\bar{\xi}$ are respectively the height of the

illuminated portion of the analyzer, the width of the illuminated portion of an identical analyzer oriented such that $\alpha = \pi/2$, the height of the detector, and the width of the detector. With the exception of $\overline{\epsilon}$, each of these lengths is to be measured in the plane of the analyzer or detector. The datum $\overline{\epsilon}$ depends on the position of Sense Switch 1 and is discussed below.

(2) The second card contains six integer fields of 3 columns each. These contain in turn the values $2\ell - 1$, $2\ell' - 1$, [defined in Eq. (5)], $N_\gamma, N_\epsilon, N_\eta, N_\xi$ [defined in Eq. (II. 1)]. Each integer is to be "right adjusted" and the first two are limited by the inequalities $2\ell - 1 \leq 9$ and $2\ell' - 1 \leq 9$.

(3) The third card is a problem-identification card which contains (up to) 72 Hollerith characters. The character in the first column controls the printer and is ordinarily "1" so that the first line of each problem is printed on a separate page.

(4) The fourth card contains six floating-point fields of width 12 in the same format as the first card. This card contains in sequence the values of $\sin\theta_1$, $\cos\theta_1$, $\sin\theta_2$, $\cos\theta_2$, $\sin\alpha$, and $\cos\alpha$. These angles are defined in Fig. 1 with $\theta_2 = \theta_R$ or $\theta_2 = -\theta_L$. Note that the integrations for the R and L detectors are treated as separate problems.

(5) This card is necessary only if Sense Switch 1 is in the "down" position. The card consists of two floating point fields of width 12 and gives the values of the lower and upper limits of the illuminated width of the analyzer, ϵ_ℓ and ϵ_μ, as measured in the plane of the analyzer. The format is the same as for the first and fourth data cards.

Two options are provided by sense switch settings in these calculations. Because the analyzer T may be skewed so that its normal makes an angle $\frac{\pi}{2} - \alpha$ with respect to the positive direction of the Z axis, the limits for the ϵ integration are ϵ_ℓ to ϵ_μ, where

$$\epsilon_\ell = - \frac{\bar{\epsilon} \ell_1}{\ell_1 \sin a - \bar{\epsilon} \cos a}$$

and

$$\epsilon_\mu = \frac{\bar{\epsilon} \ell_1}{\bar{\epsilon} \cos a + \ell_1 \sin a}$$

Here $2\bar{\epsilon}$ is the illuminated width of the analyzer in the "unskewed" position ($a = \pi/2$). For Sense Switch 1 in the "up" position, the limits ϵ_ℓ and ϵ_μ are calculated from the input datum $\bar{\epsilon}$ of card no. 1 and this fact is printed on the "output sheet." For Sense Switch 1 in the "down" position, the limits ϵ_ℓ and ϵ_μ are read into the program by means of card no. 5 and the limits calculated from the $\bar{\epsilon}$ of the first card are ignored.

For Sense Switch 2 in the "down" position, the information contained on the first two data cards of the previous calculation is retained in the memory and a new calculation is begun by reading "new" third, fourth, and possibly (depending on the setting of Sense Switch 1) fifth cards. For Sense Switch 2 in the "up" position, the reader expects an entirely new set of data beginning with a "new" first card.

The format of the "print out" is the following. The first line is the problem identification as specified by the third data card. The second lines indicates whether the ϵ limits were calculated internally or externally as provided by the position of Sense Switch 1. The third and fourth printed lines identify the calculated values of the integrals as given in the remainder of the "print out." Columnwise these values are

$$n \quad k \quad I_{n,k}(L,R) \quad \cos^n\theta_1 \cos^k\theta_2 \quad M_{n,k}(L,R) \quad \times \cos^n\theta_1 \cos^k\theta_2 \sin\theta_1 \sin\theta_2 \quad \frac{I_{n,k}}{I_{0,0}}$$

We again note that the calculations for the L and R detectors are treated as separate calculations in the FORTRAN program.

The FORTRAN listing for this program is included at the end of this Appendix.

It is possible to show that the principal error in the numerical evaluation of integrals of the form of Eq. (I. 1) is jointly proportional to the four-volume of the integration and to

$$\sum_i (r_i^4 \, \partial^4 F / \partial r_i^4)_{r_i \epsilon R} \quad ,$$

where the r_i denote the variables of integration. Instead of including a convergence test as part of the calculated program, it was felt that it would be sufficient to test this property in the following manner. The scatterer T and detectors L and R were placed so that the solid angles involved were considerably larger than practical in any experimental setup. The family of integrals $I_{n,k}$ and $M_{n,k}$ were then evaluated for the subdivision of R given by $N_\gamma = N_\epsilon = N_\eta = N_\xi = 2$. The same calculation was repeated for the subdivision given by $N_\gamma = N_\epsilon = N_\eta = N_\xi = 3$. The two sets of values obtained in this way were found to agree within "round off" although the principal error in the second calculation is only a fifth of that in the first. On the basis of this result it is concluded that the error involved in the numerical integration procedure is negligible in these calculations.

TABLE II. Input data sheet for the calculation discussed in this report. This problem is to be run with Sense Switch 1 in the "up" position and Sense Switch 2 in the "down" position.

PROGRAM 1034/PHY PROBLEM Finite Size Effects ORIGINATOR DATE PAGE OF

59.25	82.50	82.50	2.0	82.50	82.50	3.0		
3 3	2 2	2 2						
1ALPHA IS 90 DEG L1 IS 59.25 L2 IS 82.5 THETA 2 IS 45 DEG LEFT								
0. 7 7 7 1 5	0. 6 2 9 3 2	0. 7 0 7 1 1		0. 7 0 7 1 1	1. 0	0 . 0		
1ALPHA IS 90 DEG L1 IS 59.25 L2 IS 82.5 THETA 2 IS 45 DEG RIGHT								
0. 7 7 7 1 5	0. 6 2 9 3 2	0. 7 0 7 1 1		0. 7 0 7 1 1	1. 0	0. 0		

TABLE III. Output data sheet for the calculation discussed in the report: (a) for the L detector; (b) for the R detector.

(a)

ALPHA IS 90 DEG L1 IS 59.25 L2 IS 82.5 THETA 2 IS 45 DEG LEFT 332222

EPSILON LIMITS CALCULATED

POWER		CROSS SECTION		POLARIZATION		
COS1	COS2	INTEGRAL	MEAN	INTEGRAL	MEAN	
0	0	0.20284E-03	0.10000E 01	-0.11208E-03	-0.54953E 00	0.10000E 01
0	1	0.14161E-03	0.70711E 00	-0.78094E-04	-0.38858E-00	0.69814E 00
0	2	0.99020E-04	0.50000E 00	-0.54501E-04	-0.27477E-00	0.48818E-00
1	0	0.12728E-03	0.62932E 00	-0.70251E-04	-0.34583E-00	0.62752E 00
1	1	0.88931E-04	0.44500E-00	-0.48987E-04	-0.24454E-00	0.43844E-00
1	2	0.62234E-04	0.31466E-00	-0.34214E-04	-0.17292E-00	0.30682E-00
2	0	0.79923E-04	0.39604E-00	-0.44060E-04	-0.21764E-00	0.39402E-00
2	1	0.55884E-04	0.28005E-00	-0.30748E-04	-0.15389E-00	0.27551E-00
2	2	0.39138E-04	0.19802E-00	-0.21492E-04	-0.10882E-00	0.19295E-00

(b)

ALPHA IS 90 DEG L1 IS 59.25 L2 IS 82.5 THETA 2 IS 45 DEG RIGHT 332222

EPSILON LIMITS CALCULATED

POWER		CROSS SECTION		POLARIZATION		
COS1	COS2	INTEGRAL	MEAN	INTEGRAL	MEAN	
0	0	0.20284E-03	0.10000E 01	0.10978E-03	0.54953E 00	0.10000E 01
0	1	0.14161E-03	0.70711E 00	0.76585E-04	0.38858E-00	0.69814E 00
0	2	0.99020E-04	0.50000E 00	0.53515E-04	0.27477E-00	0.48818E-00
1	0	0.12716E-03	0.62932E 00	0.68844E-04	0.34583E-00	0.62689E 00
1	1	0.88709E-04	0.44500E-00	0.47994E-04	0.24454E-00	0.43734E-00
1	2	0.61986E-04	0.31466E-00	0.33513E-04	0.17292E-00	0.30559E-00
2	0	0.79763E-04	0.39604E-00	0.43201E-04	0.21764E-00	0.39324E-00
2	1	0.55606E-04	0.28005E-00	0.30096E-04	0.15389E-00	0.27414E-00
2	2	0.38827E-04	0.19802E-00	0.21000E-04	0.10882E-00	0.19142E-00

TABLE IV. FORTRAN Listing

```
C      1034/PHY  CORRECTION TO RIGHT-LEFT ASYMMETRY          ELWYN MONAHAN
       DIMENSION X1(3),Y1(3),Z1(3),X2(3),Y2(3),Z2(3),F1(3,3,3),F2(3,3,3),
      XF3(3,3,3),G1(3,3,3),G2(3,3,3),G3(3,3,3),ANSCS(10,10),ANSPOL(10,10)
      X,R1(3,3),RR1(3,3,3),RR2(3,3,3),RR3(3,3,3),T1(3,3),TT1(3,3,3),
      XII2(3,3,3),II3(3,3,3)
    10 FORMAT(72H1
      X                    )
    20 FORMAT(6F12.6)
    30 FORMAT(6I3)
    40 FORMAT(54HO    POWER          CROSS  SECTION                POLARIZATION)
C
    50 FORMAT(55HOCOS1    COS2    INTEGRAL          MEAN        INTEGRAL    MEAN)
    60 FORMAT(1HO2I4,5E14.5)
   407 FORMAT(23HOEPSILON LIMITS READ IN)
   411 FORMAT(26HOEPSILON LIMITS CALCULATED)
C
  1111 READ 20, D1,D2,GBAR,EBAR,ETABAR,XIBAR
       READ 30, N1CS,N2CS,NGIL,NEIL,NETAIL,NXIIL
C
     1 READ 10
       READ 20, S1I,C1I,S2I,C2I,SALPHA,CALPHA
C
C
   400 IF(SENSESWITCH1)401,403
   401 READ20,EBARL,EBARU
   402 GOTO405
   403 EBARL=(EBAR*D1)/(D1*SALPHA-EBAR*CALPHA)
   404 EBARU=(EBAR*D1)/(D1*SALPHA+EBAR*CALPHA)
   405 CONTINUE
   201 ONGIL=NGIL
   202 ONEIL=NEIL
   203 ONETAL=NETAIL
   204 ONXIIL=NXIIL
   205 HG=GBAR/ONGIL
   206 HE=(EBARU+EBARL)/(2.0*ONEIL)
   207 HETA=ETABAR/ONETAL
   208 HXI=XIBAR/ONXIIL
C
   209 DO1000N1=1,N1CS
   210 DO1000N2=1,N2CS
   211 ANSCS(N1,N2)=0.0
   212 ANSPOL(N1,N2)=0.0
C
   213 DO1010L=1,NGIL
   214 DO1010M=1,NEIL
   215 DO1010N=1,NETAIL
   216 DO1010KK=1,NXIIL
   217 OL=L
   218 OM=M
   219 ON=N
   220 OK=KK
   221 GO=((2.0*(OL-1.0)/ONGIL)-1.0)*GBAR
   222 EO=((OM-1.0)*(EBARU+EBARL))/CNEIL-EBARL
   223 ETAO=((2.0*(ON-1.0)/ONETAL)-1.0)*ETABAR
   224 XIO=((2.0*(OK-1.0)/ONXIIL)-1.0)*XIBAR
C
   225 DO1020J=1,3
   226 OJ=J
   227 X1(J)=GO+HG*(OJ-1.0)
   228 Y1(J)=(EO+HE*(OJ-1.0))*SALPHA
   229 Z1(J)=D1-(EO+HE*(OJ-1.0))*CALPHA
```

TABLE IV. FORTRAN Listing (Cont'd)

```
      X2(J)=ETAO+HETA*(OJ-1.0)
      Y2(J)=D2*S2T+(XIO+HXI*(OJ-1.0))*C2T
 1020 Z2(J)=D1+D2*C2T-(XIO+HXI*(OJ-1.0))*S2T
C
      DO1030J=1,3
      DO1030K=1,3
      AUX=X1(J)**2+Y1(K)**2+Z1(K)**2
      R1(J,K)=SQRTF(AUX)
 1030 T1(J,K)=(Z1(K)*C1T-Y1(K)*S1T)/R1(J,K)
C
      DO1040I=1,3
      DO1040J=1,3
      DO1040K=1,3
      AUX3=(Y2(K)-Y1(I))**2+(Z2(K)-Z1(I))**2
      AUX=(X2(J)-X1(1))**2+AUX3
      RR1(I,J,K)=SQRTF(AUX)
      AUX=(X2(J)-X1(2))**2+AUX3
      RR2(I,J,K)=SQRTF(AUX)
      AUX=(X2(J)-X1(3))**2+AUX3
      RR3(I,J,K)=SQRTF(AUX)
      AUX3=Y1(I)*(Y2(K)-Y1(I))+Z1(I)*(Z2(K)-Z1(I))
      AUX=X1(1)*(X2(J)-X1(1))+AUX3
      TT1(I,J,K)=AUX/(R1(1,I)*RR1(I,J,K))
      AUX=X1(2)*(X2(J)-X1(2))+AUX3
      TT2(I,J,K)=AUX/(R1(2,I)*RR2(I,J,K))
      AUX=X1(3)*(X2(J)-X1(3))+AUX3
      TT3(I,J,K)=AUX/(R1(3,I)*RR3(I,J,K))
C
      AUX1=(Y2(K)-Y1(I))*S2T+(Z2(K)-Z1(I))*C2T
      AUX=(Y1(I)*CALPHA+Z1(I)*SALPHA)*AUX1
      F1(I,J,K)=AUX/((R1(1,I)**3)*(RR1(I,J,K)**3))
      F2(I,J,K)=AUX/((R1(2,I)**3)*(RR2(I,J,K)**3))
      F3(I,J,K)=AUX/((R1(3,I)**3)*(RR3(I,J,K)**3))
C
      IF(N1-1)2,3,?
    2 NAUX=N1-1
      F1(I,J,K)=F1(I,J,K)*(T1(1,I)**NAUX)
      F2(I,J,K)=F2(I,J,K)*(T1(2,I)**NAUX)
      F3(I,J,K)=F3(I,J,K)*(T1(3,I)**NAUX)
    3 IF(N2-1)4,5,4
    4 NAUX=N2-1
      F1(I,J,K)=F1(I,J,K)*(TT1(I,J,K)**NAUX)
      F2(I,J,K)=F2(I,J,K)*(TT2(I,J,K)**NAUX)
      F3(I,J,K)=F3(I,J,K)*(TT3(I,J,K)**NAUX)
    5 CONTINUE
      AUX=Y1(I)*CALPHA+Z1(I)*SALPHA
      F1(I,J,K)=F1(I,J,K)*R1(1,I)/AUX
      F2(I,J,K)=F2(I,J,K)*R1(2,I)/AUX
      F3(I,J,K)=F3(I,J,K)*R1(3,I)/AUX
C
      AUX1=(Z1(I)*Y2(K)-Y1(I)*Z2(K))*(Z1(I)*S1T+Y1(I)*C1T)
      AUX=AUX1+(Z1(I)*X2(J)-X1(1)*Z2(K))*X1(1)*C1T
      AUX=AUX+(X1(1)*Y2(K)-Y1(I)*X2(J))*X1(1)*S1T
      G1(I,J,K)=(AUX*F1(I,J,K))/((R1(1,I)**2)*RR1(I,J,K))
      AUX=AUX1+(Z1(I)*X2(J)-X1(2)*Z2(K))*X1(2)*C1T
      AUX=AUX+(X1(2)*Y2(K)-Y1(I)*X2(J))*X1(2)*S1T
      G2(I,J,K)=(AUX*F2(I,J,K))/((R1(2,I)**2)*RR2(I,J,K))
      AUX=AUX1+(Z1(I)*X2(J)-X1(3)*Z2(K))*X1(3)*C1T
      AUX=AUX+(X1(3)*Y2(K)-Y1(I)*X2(J))*X1(3)*S1T
 1040 G3(I,J,K)=(AUX*F3(I,J,K))/((R1(3,I)**2)*RR3(I,J,K))
C
      CALLSUMMAD(F1,F2,F3,SUM)
```

TABLE IV. FORTRAN Listing (Cont'd)

```
      ANSCS(N1,N2)=ANSCS(N1,N2)+SUM
      CALLSUMMAD(G1,G2,G3,SUM)
 1010 ANSPOL(N1,N2)=ANSPOL(N1,N2)+SUM
C
      AUX=HG*HE*HETA*HXI
      ANSCS(N1,N2)=AUX*ANSCS(N1,N2)
 1000 ANSPOL(N1,N2)=AUX*ANSPOL(N1,N2)
C
      PRINT10
      IF(SENSESWITCH1)408,410
      PRINT407
      GOTO412
      PRINT411
      CONTINUE
      PRINT40
      PRINT50
C
      DO11N1=1,N1CS
      N=N1-1
      IF(N)423,421,423
      XC1=1.0
      GOTO424
      XC1=C1T**N
      CONTINUE
      DO11N2=1,N2CS
      M=N2-1
      IF(M)428,426,428
      XC2=1.0
      GOTO286
      XC2=C2T**M
      XC=XC1*XC2
      XP=XC*S1T*S2T
      XYZ=ANSCS(N1,N2)/ANSCS(1,1)
      PRINT60,N,M,ANSCS(N1,N2),XC,ANSPOL(N1,N2),XP,XYZ
   11 CONTINUE
      IF(SENSESWITCH2)289,1111
      GOTO1
      END(0,1,0,0,1)
    1 SUBROUTINESUMMAD(F1,F2,F3,SUM)
      DIMENSIONF1(3,3,3),F2(3,3,3),F3(3,3,3)
    2 A=0.0
    3 DO6J=1,3,2
    4 DO6K=1,3,2
    5 DO6L=1,3,2
    6 A=A+F1(J,K,L)+F3(J,K,L)
    7 B=4.0*(F1(1,1,2)+F1(1,2,1)+F1(2,1,1)+F1(1,2,3)+F1(1,3,2)+F1(2,1,3)
      X+F1(2,3,1)+F1(3,1,2)+F1(3,2,1)+F1(2,3,3)+F1(3,2,3)+F1(3,3,2))
    8 B=B+4.0*(F2(1,1,1)+F2(1,1,3)+F2(1,3,1)+F2(3,1,1)+
      XF2(1,3,3)+F2(3,1,3)+F2(3,3,1)+F2(3,3,3))
    9 B=B+4.0*(F3(1,1,2)+F3(1,2,1)+F3(2,1,1)+F3(1,2,3)+F3(1,3,2)+
      XF3(2,1,3)+F3(2,3,1)+F3(3,1,2)+F3(3,2,1)+F3(2,3,3)+F3(3,2,3)+
      XF3(3,3,2))
   10 C=16.0*(F1(1,2,2)+F1(2,1,2)+F1(2,2,1)+F2(1,1,2)+F2(1,2,1)+
      XF2(2,1,1)+F1(2,2,3)+F1(2,3,2)+F1(3,2,2)+F2(1,2,3)+F2(1,3,2)+
      XF2(2,3,1)+F2(3,1,2)+F2(3,2,1)+F3(1,2,2)+F3(2,1,2)+F3(2,2,1)+
      XF2(2,1,3)+F2(2,3,3)+F2(3,2,3)+F2(3,3,2)+F3(2,2,3)+F3(2,3,2)+
      XF3(3,2,2))
   11 D=64.0*(F1(2,2,2)+F2(1,2,2)+F2(2,1,2)+F2(2,2,3)+
      XF2(2,3,2)+F2(3,2,2)+F3(2,2,2)+F2(2,2,1))
   12 E=256.0*F2(2,2,2)
   13 SUM=(A+B+C+D)/81.0
C
   14 RETURN
   15 END(0,1,0,0,1)
```

REFERENCES

[1]See for example T. A. Welton, in Fast Neutron Physics, edited by J. B. Marion and J. L. Fowler (Interscience Publishers, Inc., New York, in press), Part II, Chap. V. F and W. Haeberli, ibid, Part II, Chap. V. G for a list of references.

[2]"The Basel Convention", Proceedings of the International Symposium on Polarization Phenomena of Nucleons, Helv. Phys. Acta, Supplement VI, 436 (1961).

[3]J. E. Evans, United Kingdom Atomic Energy Authority Report AERE-R3347 (1960).

[4]A. Langsdorf, Jr., R. O. Lane, and J. E. Monahan, Phys. Rev. 107, 1077 (1957); R. O. Lane, A. S. Langsdorf, Jr., J. E. Monahan, and A. J. Elwyn, Ann. Phys. 12, 135 (1961).

[5]A. J. Elwyn and R. O. Lane (to be published).

[6]A. J. Elwyn, R. O. Lane, and A. Langsdorf, Jr. (to be published).

[7]S. M. Austin, S. E. Darden, A. Okazaki, and Z. Wilhelmi, Nuclear Phys. 22, 451 (1961); S. E. Darden, T. R. Donoghue, and C. A. Kelsey, Nuclear Phys. 22, 439 (1961).